heterozygous for S2889X、患者 2：compound heterozygous for 3321delA and S2889X、患者 3：heterozygous for S3296X、患者 4：変異なし）を有していたのに対し、3 人の内因性 AD 患者はいずれのフィラグリン遺伝子変異も有していなかった。末梢血中 Th2 細胞、Th17 細胞割合は、外因性と内因性間で有意差は無かったが、Th1 細胞割合は内因性 AD 患者で増加していた。

D．考察

ADに続発する気管支喘息とフィラグリン遺伝子変異との間に有意な相関関係が認められた。また、現時点での症例数は少ないものの、外因性ADとフィラグリン遺伝子変異との間に正の相関関係がある可能性が高く、これはフィラグリン遺伝子変異に伴う表皮バリア障害が、アレルギー性である外因性ADの発症に大きく関わっていることを示唆している。さらに、Th2細胞とTh17細胞をアレルギー発症の主体とする外因性ADはバリア障害に基づく蛋白抗原の曝露が関与し、Th1細胞がより関わる内因性ADでは蛋白抗原以外の抗原、例えば金属等が発症に関わっている可能性も示唆された。

E．結論

フィラグリン遺伝子変異に伴う表皮バリア機能を改善することで AD のみならず、AD に続発する気管支喘息の発症を予防できる可能性が高いものと考えられ、症例のさらなる集積を目指していく。

F．健康危険情報

特になし。

G．研究発表

Osawa R, Konno S, Akiyama M, Nemoto-Hasebe I, Nomura T, Abe R, Sandilands A, McLean WHI, Hizawa N, Nishimura M, Shimizu H:
Japanese-specific filaggrin gene mutations are a major risk factor for atopic eczema with asthma in the Japanese population.
J Allergy Clin Immunol（論文投稿中）

H．知的財産の出願・登録状況

特になし。

	R501X		3321delA		S1695X		Q1701X		S2554X		S2889X		S3296X		K4022X		Combined			
Genotypes	Con	Asthma	Cont	Asthma	Con	Asthma	Con	Asthma	Con	Asthma	Con	Asthma	Con	Asthma	Con	Asthma	Con	Asthma (total)	Asthma (AE+)	Asthma (AE−)
AA	134	105	133	105	133	105	134	105	133	102	132	101	134	105	134	105	129	98	11	87
Aa	0	0	1	0	1	0	0	0	1	3	2	4	0	0	0	0	5	7	2	5
aa	0	0	0	0	0	0	0	0	0	0	0	0	0	0	0	0	0	0	0	0
total	134	105	134	105	134	105	134	105	134	105	134	105	134	105	134	105	134	105	13	92

AE, atopic eczema; Con, healthy controls

For combined genotype: Asthma+AE, Fisher's exact test P=0.118, Fisher's exact test odds ratio=4.69 (95% CI 0.81-27.04);

Asthma-AE, Fisher's exact test P=0.744, Fisher's exact test odds ratio=1.48 (95% CI 0.42-5.28);

All Asthma, Fisher's exact test P=0.376, Fisher's exact test odds ratio=1.84 (95% CI 0.57-5.98)

図５．日本人気管支喘息患者とフィラグリン遺伝子変異

AD に続発する気管支喘息とフィラグリン遺伝子変異との間に有意な相関関係が認められた。

Ⅳ．研究成果の刊行に関する一覧表

研究成果の刊行に関する一覧表（雑誌）

発表者氏名	論文タイトル名	発表雑誌	巻号	ページ	出版年
Wang G, Ujiie H, Shibaki A, Nishie W, Tateishi Y, Kikuchi K, Li Q, McMillan JR, Morioka H, Sawamura D, Nakamura H, Shimizu H	Blockade of autoantibody-initiated tissue damage by using recombinant Fab antibody fragments against pathogenic autoantigen	**Am J Patho l**			in press
Ujiie H, Shibaki A, Nishie W, Sawamura D, Wang G, Tateishi Y, Li Q, Moriuchi R, Qiao H, Nakamura H, Akiyama M, Shimizu H	A novel active mouse model for bullous pemphigoid targeting humanized pathogenic antigen	**J Immunol**			in press
Ujiie H, Shibaki A, Akiyama M, Shimizu H	Successful treatment of nail lichen planus with topical tacrolimus	**Acta Derm Venereol**			in press
Ujiie H, Kodama K, Akiyama M, Shimizu H	Hereditary benign telangiectasia: Two families with punctate telangiectasias surrounded by anemic halos	**Arch Dermatol**			in press
Natsuga K, Sawamura D, Goto M, Homma E, Goto-Ohguchi Y, Aoyagi S, Akiyama M, Kuroyanagi Y, Shimizu H	Response of intractable skin ulcers in recessive dystrophic epidermolysis bullosa patients to an allogeneic cultured dermal substitute	**Acta Derm Venereol**			in press
Natsuga K, Nishie W, Shinkuma S, Moriuchi R, Shibata M, Nishimura M, Hashimoto T, Shimizu H	Circulating IgA and IgE autoantibodies in antilaminin-332 mucous membrane pemphigoid	**Br J Dermatol**			in press
Natsuga K, Nishie W, Akiyama M, Nakamura H, Shinkuma S, McMillan JR, Nagasaki A, Has C, Ouchi T, Ishiko A, Hirako Y, Owaribe K, Sawamura D, Bruckner-Tuderman L, Shimizu H	Plectin expression patterns determine two distinct subtypes of epidermolysis bullosa simplex	**Hum Mutat**			in press
Inokuma D, Shibaki A, Shimizu H	Two cases of cutaneous sporotrichosis in continental/ microthermal climate zone: global warming alert?	**Clin Exp Dermatol**			in press
Iitani MM, Abe R, Yanagi T, Hamasaka A, Tateishi Y, Abe Y, Ito M, Kondo T, Kubota K, Shimizu H	Aleukemic leukemia cutis with extensive bone involvement	**J Am Acad Dermatol**			in press

Aoyagi S, Hata H, Homma E, Shimizu H	Controlling the histological margin for non-melanoma skin cancer conveniently using a double-bladed scalpel	**J Surg Oncol**			in press
Ando S, Sato-Matsumura K, Kasai M, Nemoto-Hasebe I, Hoshina D, Ohyama B, Hashimoto T, Shimizu H	Desmoglein1 and bullous pemphigoid 180 ELISA indexes correlating with disease activity in a patient with coexisting pemphigus foliaceus and bullous pemphigoid	**Clin Exp Dermatol**			in press
Mori T, Ishida K, Mukumoto S, Yamada Y, Imokawa G, Kabashima K, Kobayashi M, Bito T, Nakamura M, Ogasawara K, Tokura Y	Comparison of skin barrier function and sensory nerve electric current perception threshold between IgE-high extrinsic and IgE-normal intrinsic types of atopic dermatitis	**Br J Dermatol**			in press
Ine K-I, Kabashima K, Koga C, Kobayashi M, Tokura Y	Eruptive generalized granuloma annulare presenting with numerous micropapules	**Int J Dermatol**			in press
Tomura M, Honda T, Tanizaki H, Otsuka A, Egawa G, Tokura Y, Hori S, Miyachi Y, Kanagawa O, Kabashima K	Activated Regulatory T cells are the major T cell type emigrating from sensitized skin	**J Clin Invest**			in press
Moniaga CS, Egawa G, Kawasaki H, Chikuma M, Honda T, Tanizaki H, Nakajima S, Matsuoka H, Kubo A, Tokura Y, Miyachi Y, Amagai M, Kabashima K	Flaky tail mouse denotes human atopic dermatitis in the steady state and by topical application with Dermatophagoides pteronyssimus extract	**Am J Pathol**			in press
Yoshiki R, Kabashima K, Sakabe J-I, Sugita K, Bito T, Nakamura M, Malissen B, Tokura Y	The mandatory role of IL-10-producing and OX40L-expresssing mature Langerhans cells in local UVB-induced immunosuppression	**J Immunol**			in press
Shimauchi T, Sugita K, Nakamura M, Tokura Y	Leukemic cutaneous T-cell lymphoma manifesting papuloerythroderma with CD3- CD4+ phenotype	**Acta Derma Venereol**	90	68-72	2010
Yanagi T, Shimizu T, Kodama K, Nemoto-Hasebe I, Kasai M, Shimizu H	CD30-positive primary cutaneous anaplastic large-cell lymphoma and definite squamous cell carcinoma	**Clin Exp Dermatol**	34	e293-294	2009
Ujiie H, Akiyama M, Osawa R, Shida S, Aoyagi S, Shimizu H	Bloody nipple discharge in an infant	**Arch Dermatol**	145	1068-1069	2009

Suzuki K, Yamaguchi Y, Villacorte M, Mihara K, Akiyama M, Shimizu H, Taketo MM, Nakagata N, Tsukiyama T, Yamaguchi TP, Birchmeier W, Kato S, Yamada G	Embryonic hair follicle fate change by augmented {beta}-catenin through Shh and Bmp signaling	**Development**	136	367-372	2009
Shinkuma S, Akiyama M, Torii-Saito N, Natsuga K, Tateishi Y, Ito K, Hirota J, Shimizu Y, Shichinohe T, Shimizu H	Pemphigus foliaceus associated with oesophageal cancer	**J Eur Acad Dermatol Venereol**	23	473-474	2009
Shinkuma S, Abe R, Nishimura M, Natsuga K, Fujita Y, Nomura T, Nishie W, Shimizu H	Secondary syphilis mimicking warts in an HIV-positive patient	**Sex Transm Infect**	85	484	2009
Sakai K, Akiyama M, Yanagi T, McMillan JR, Suzuki T, Tsukamoto K, Sugiyama H, Hatano Y, Hayashitani M, Takamori K, Nakashima K, Shimizu H	ABCA12 is a major causative gene for non-bullous congenital ichthyosiform erythroderma	**J Invest Dermatol**	129	2306-2309	2009
Qiao H, Shibaki A, Long HA, Wang G, Li Q, Nishie W, Abe R, Akiyama M, Shimizu H, McMillan JR	Collagen XVII participates in keratinocyte adhesion to collagen IV, and in p38MAPK-dependent migration and cell signaling	**J Invest Dermatol**	129	2288-2295	2009
Osawa R, Akiyama M, Yamanaka Y, Ujiie H, Nemoto-Hasebe I, Takeda A, Yanagi T, Shimizu H	A novel PTPN11 missense mutation in a patient with LEOPARD syndrome	**Br J Dermatol**	161	1202-1204	2009
Nomura Y, Nishie W, Shibaki A, Ibata M, Shimizu H	Disseminated cutaneous Mycobacterium kansasii infection in an patient infected with the human immunodeficiency virus	**Clin Exp Dermatol**	34	625-626	2009
Nomura Y, Akiyama M, Nishie W, Shimizu H	Progressive Refractory Ulcer of the Nipple: A Quiz	**Acta Derm Venereol**	89	445-447	2009
Nomura Y, Abe M, Natsuga K, Moriuchi R, Kawasaki H, Mayuzumi M, Yasuoka A, Shimizu H	Widespread keratosis follicularis squamosa	**Clin Exp Dermatol**	34	519-520	2009
Nomura T, Akiyama M, Sandilands A, Nemoto-Hasebe I, Sakai K, Nagasaki A, Palmer CN, Smith FJ, McLean WH, Shimizu H	Prevalent and rare mutations in the gene encoding filaggrin in Japanese patients with ichthyosis vulgaris and atopic dermatitis	**J Invest Dermatol**	129	1302-1305	2009
Nishie W, Sawamura D, Natsuga K, Shinkuma S, Goto M, Shibaki A, Ujiie H, Olasz E, Yancey KB, Shimizu H	A novel humanized neonatal autoimmune blistering skin disease model induced by maternally transferred antibodies	**J Immunol**	183	4088-4093	2009

Nemoto-Hasebe I, Akiyama M, Nomura T, Sandilands A, McLean WH, Shimizu H	FLG mutation p.Lys4021X in the C-terminal imperfect filaggrin repeat in Japanese patients with atopic eczema	**Br J Dermatol**	161	1387-1390	2009
Nemoto-Hasebe I, Akiyama M, Nomura T, Sandilands A, McLean WH, Shimizu H	Clinical severity correlates with impaired barrier in filaggrin-related eczema	**J Invest Dermatol**	129	682-689	2009
Nemoto-Hasebe I, Akiyama M, Kudo S, Ishiko A, Tanaka A, Arita K, Shimizu H	Novel mutation p.Gly59Arg in GJB6 encoding connexin 30 underlies palmoplantar keratoderma with pseudoainhum, knuckle pads and hearing loss	**Br J Dermatol**	161	452-455	2009
Natsuga K, Shinkuma S, Nishie W, Shimizu H	Animal models of epidermolysis bullosa	**Dermatol Clin**	28	137-142	2009
Long HA, McMillan JR, Qiao H, Akiyama M, Shimizu H	Current advances in gene therapy for the treatment of genodermatoses	**Curr Gene Ther**	9	487-494	2009
Kawabori M, Kuroda S, Nakayama N, Kenmotsu Y, Shimizu H, Tanino M, Iwasaki Y	Spontaneous giant aneurysm of the superficial temporal artery: case report	**Neurol Med Chir**	49	198-201	2009
Kanda M, Natsuga K, Nishie W, Akiyama M, Nagasaki A, Shimizu T, Shimizu H	Morphological and genetic analysis of steatocystoma multiplex in an Asian family with pachyonychia congenita type 2 harbouring a KRT17 missense mutation	**Br J Dermatol**	160	465-468	2009
Ito K, Sawamura D, Goto M, Nakamura H, Nishie W, Sakai K, Natsuga K, Shinkuma S, Shibaki A, Uitto J, Denton CP, Nakajima O, Akiyama M, Shimizu H	Keratinocyte-/fibroblast-targeted rescue of Col7a1-disrupted mice and generation of an exact dystrophic epidermolysis bullosa model using a human COL7A1 mutation	**Am J Pathol**	175	2508-2517	2009
Inomata K, Aoto T, Binh NT, Okamoto N, Tanimura S, Wakayama T, Iseki S, Hara E, Masunaga T, Shimizu H, Nishimura EK	Genotoxic stress abrogates renewal of melanocyte stem cells by triggering their differentiation	**Cell**	137	1088-1099	2009
Inokuma D, Sawamura D, Shibaki A, Abe R, Shimizu H	Scleroedema adultorum associated with sarcoidosis	**Clin Exp Dermatol**	34	e428-429	2009
Inokuma D, Kodama K, Natsuga K, Kasai M, Abe M, Nishie W, Abe R, Hashimoto T, Shimizu H	Autoantibodies against type XVII collagen C-terminal domain in a patient with bullous pemphigoid associated with psoriasis vulgaris	**Br J Dermatol**	160	451-454	2009
Inokuma D, Aoyagi S, Saito N, Iitani MM, Homma E, Hamasaka K, Shimizu H	Bowen's disease of the nail matrix presenting as melanonychia: detection of human papillomavirus type 56	**Acta Derm Venereol**	89	638-639	2009

Imada K, Dainichi T, Yokomizo A, Tsunoda T, Song YH, Nagasaki A, Sawamura D, Nishie W, Shimizu H, Fukagawa S, Urabe K, Furue M, Hashimoto T, Naito S	Birt-Hogg-Dube syndrome with clear-cell and oncocytic renal tumour and trichoblastoma associated with a novel FLCN mutation	**Br J Dermatol**	160	1350-1353	2009
Hsu CK, Akiyama M, Nemoto-Hasebe I, Nomura T, Sandilands A, Chao SC, Lee JY, Sheu HM, McLean WH, Shimizu H	Analysis of Taiwanese ichthyosis vulgaris families further demonstrates differences in FLG mutations between European and Asian populations	**Br J Dermatol**	161	448-451	2009
Honda A, Abe R, Yoshihisa Y, Makino T, Matsunaga K, Nishihira J, Shimizu H, Shimizu T	Deficient deletion of apoptotic cells by macrophage migration inhibitory factor (MIF) overexpression accelerates photocarcinogenesis	**Carcinogenesis**	30	1597-1605	2009
Hamasaka E, Akiyama M, Hata H, Aoyagi S, Shimizu H	Melanonychia caused by Stenotrophomonas maltophilia	**Clin Exp Dermatol**	34	242-243	2009
Hamasaka A, Abe R, Koyama Y, Yoshioka N, Fujita Y, Hoshina D, Sasaki M, Hirasawa T, Onodera S, Ohshima S, Leng L, Bucala R, Nishihira J, Shimizu T, Shimizu H	DNA vaccination against macrophage migration inhibitory factor improves atopic dermatitis in murine models	**J Allergy Clin Immunol**	124	90-99	2009
Goto-Ohguchi Y, Nishie W, Akiyama M, Tateishi Y, Aoyagi S, Tsuji-Abe Y, Sawamura D, Ishii N, Hashimoto T, Shimizu H	A severe and refractory case of anti-p200 pemphigoid resulting in multiple skin ulcers and scar formation	**Dermatology**	218	265-271	2009
Bohgaki T, Atsumi T, Bohgaki M, Furusaki A, Kondo M, Sato-Matsumura KC, Abe R, Kataoka H, Horita T, Yasuda S, Amasaki Y, Nishio M, Sawada K, Shimizu H, Koike T	Immunological reconstitution after autologous hematopoietic stem cell transplantation in patients with systemic sclerosis: relationship between clinical benefits and intensity of immunosuppression	**J Rheumatol**	36	1240-1248	2009
Asaka T, Akiyama M, Kitagawa Y, Shimizu H	Higher density of label-retaining cells in gingival epithelium	**J Dermatol Sci**	55	132-134	2009
Asaka T, Akiyama M, Domon T, Nishie W, Natsuga K, Fujita Y, Abe R, Kitagawa Y, Shimizu H	Type XVII collagen is a key player in tooth enamel formation	**Am J Pathol**	174	91-100	2009
Aoyagi S, Izumi K, Hata H, Kawasaki H, Shimizu H	Usefulness of real-time tissue elastography for detecting lymph-node metastases in squamous cell carcinoma	**Clin Exp Dermatol**	34	e744-e747	2009

Aoyagi S, Hata H, Iitani MM, Homma E, Inokuma D, Shimizu H	Squamous cell carcinoma of the auricle with rhabdoid features	**J Cutan Pathol**	36	919-921	2009
Ando S, Abe R, Sasaki M, Murata J, Inokuma D, Shimizu H	Bone marrow-derived cells are not the origin of the cancer stem cells in ultraviolet-induced skin cancer	**Am J Pathol**	174	595-560	2009
Akiyama M, Sakai K, Hayasaka K, Tabata N, Yamada M, Ujiie H, Shibaki A, Shimizu H	Conradi-Hunermann-Happle syndrome with abnormal lamellar granule contents	**Br J Dermatol**	160	1335-1337	2009
Abe R, Yoshioka N, Murata J, Fujita Y, Shimizu H	Granulysin as a marker for early diagnosis of the Stevens-Johnson syndrome	**Ann Intern Med**	151	514-515	2009
Amagai M, Ikeda S, Shimizu H, Iizuka H, Hanada K, Aiba S, Kaneko F, Izaki S, Tamaki K, Ikezawa Z, Takigawa M, Seishima M, Tanaka T, Miyachi Y, Katayama I, Horiguchi Y, Miyagawa S, Furukawa F, Iwatsuki K, Hide M, Tokura Y, Furue M, Hashimoto T, Ihn H, Fujiwara S, Nishikawa T, Ogawa H, Kitajima Y, Hashimoto K	A randomized double-blind trial of intravenous immunoglobulin for pemphigus	**J Am Acad Dermatol**	60	595-603	2009
Kobayashi M, Yoshiki R, Sakabe J, Kabashima K, Nakamura M, Tokura Y	Expression of toll-like receptor 2, NOD2 and dectin-1 and stimulatory effects of their ligands and histamine in normal human keratinocytes	**Br J Dermatol**	160	297-304	2009
Yoshiki R, Kabashima K, Sugita K, Atarashi K, Shimauchi T, Tokura Y	IL-10-Producing Langerhans Cells and Regulatory T Cells Are Responsible for Depressed Contact Hypersensitivity in Grafted Skin	**J Invest Dermatol**	129	705-713	2009
Nakamura M, Tokura Y	Congenital woolly hair without P2RY5 mutation	**Dermato-Endocrinology**	1	58-59	2009
Fukamachi S, Nakamura M, Tokura Y	Cisplatin-induced acral erythema	**Eur J Dermatol**	19	171-172	2009
Fukamachi S, Kabashima K, Sugita K, Kobayashi M, Tokura Y	Therapeutic effectiveness of various treatments for eosinophilic pustular folliculitis	**Acta Derm Venereol**	89	155-159	2009
Atarashi K, Mori T, Yoshiki R, Kabashima K, Kuma H, Tokura Y	Skin application of ketoprofen systemically suppresses contact hypersensitivity by inducing CD4(+) CD25(+) regulatory T cells	**J Dermatol Sci**	53	216-221	2009

Sakabe JI, Nakamura M, Tokura Y	A missense mutation in exon 1 of the keratin 9 gene in a Japanese patient with "Vörner type" hereditary palmoplantar keratoderma	**Eur J Dermatol**	19	286-287	2009
Nishio D, Nakashima D, Mori T, Kabashima K, Tokura Y	Induction of eosinophil-infiltrating drug eruption in mice	**J Dermtol Sci**	55	34-39	2009
Tokura Y	Greeting from the President of the Japanese Society for Investigative Dermatology (JSID) On achieving internationalization and educating young researchers	**J Dermatol Sci**	54	141-142	2009
Sakabe JI, Kabashima K, Sugita K, Tokura Y	Possible involvement of T lymphocytes in the pathogenesis of Nagashima-type keratosis palmoplantaris	**Clin Exp Dermatol**	34	e282-284	2009
Isoda H, Kabashima K, Tokura Y	'Nagashima-type' keratosis palmoplantaris in two siblings	**J Eur Acad Dermatol Venereol**	23	737-738	2009
Sugita K, Shimauchi T, Kabashima R, Nakashima D, Hino R, Kabashima K, Nakamura M, Tokura Y	Loss of tumor cell CCR4 expression upon leukemic change in adult T-cell leukemia/lymphoma	**J Am Acad Dermatol**	61	163-164	2009
Ine K, Kabashima K, Koga C, Kobayashi M, Tokura Y	Mixed tumor of the skin arising on the auricle	**J Dermatol**	36	1-3	2009
Onoue A, Kabashima K, Kobayashi M, Mori T, Tokura Y	Induction of eosinophil- and Th2-attracting epidermal chemokines and cutaneous late-phase reaction in tape-stripped skin	**Exp Dermatol**	18	1036-1043	2009
Kobayashi M, Kabashima K, Nakamura M, Tokura Y	Effects of oral antibiotic roxithromycin on quality of life in acne patients	**J Dermatol**	36	383-391	2009
Kabashima R, Kabashima K, Mukumoto S, Hino R, Huruno Y, Kabashima N, Tokura Y	Kimura's disease presenting with a giant suspensory tumor and associated with membranoproliferative glomerulonephritis	**Eur J Dermatol**	19	626-628	2009
Sugita K, Kabashima K, Yoshiki R, Ikenouchi-Sugita A, Tsutsui M, Nakamura J, Yanagihara N, Tokura Y	Inducible Nitric Oxide Synthase Downmodulates Contact Hypersensitivity by Suppressing Dendritic Cell Migration and Survival	**J Invest Dermatol**	130	464-471	2009
Kato M, Ohshima K, Mizuno M, Kyogoku M, Hashikawa K, Tokura Y, Miyachi Y, Kabashima K	Analysis of CXCL9 and CXCR3 expression in a case of intravascular large B-cell lymphoma	**J Am Acad Dermatol**	61	888-891	2009
Sugita K, Kobayashi M, Mori T, Kabashima K, Nakamura M, Tokura Y	Antihistaminic drug olopatadine downmodulates CCL17/TARC production by keratinocytes and Langerhans cells	**J Dermatol**	36	654–657	2009

Sugita K, Kabashima K, Nakamura M, Tokura Y	Drug-induced Papuloerythroderma: Analysis of T-cell Populations and a Literature Review	**Acta Derm Venereol**	89	618-622	2009

Ⅴ．研究成果の刊行物・別刷

The American Journal of Pathology, Vol. 176, No. 2, February 2010

DOI: 10.2353/ajpath.2010.090744

Stem Cells, Tissue Engineering and Hematopoietic Elements

Blockade of Autoantibody-Initiated Tissue Damage by Using Recombinant Fab Antibody Fragments against Pathogenic Autoantigen

Gang Wang,*† Hideyuki Ujiie,* Akihiko Shibaki,* Wataru Nishie,* Yasuki Tateishi,* Kazuhiro Kikuchi,* Qiang Li,* James R. McMillan,*† Hiroshi Morioka,‡ Daisuke Sawamura,* Hideki Nakamura,* and Hiroshi Shimizu*

From the Department of Dermatology, Hokkaido University Graduate School of Medicine, the Creative Research Initiative Sousei,† and the Faculty of Pharmaceutical Sciences,‡ Hokkaido University, Sapporo, Japan*

Activation of the complement cascade via the classical pathway is required for the development of tissue injury in many autoantibody-mediated diseases. It therefore makes sense to block the pathological action of autoantibodies by preventing complement activation through inhibition of autoantibody binding to the corresponding pathogenic autoantigen using targeted Fab antibody fragments. To achieve this, we use bullous pemphigoid (BP) as an example of a typical autoimmune disease. Recombinant Fabs against the non-collagenous 16th-A domain of type XVII collagen, the main pathogenic epitope for autoantibodies in BP, were generated from antibody repertoires of BP patients by phage display. Two Fabs, Fab-B4 and Fab-19, showed marked ability to inhibit the binding of BP autoantibodies and subsequent complement activation *in vitro*. In the *in vivo* experiments using type XVII collagen humanized BP model mice, these Fabs protected mice against BP autoantibody-induced blistering disease. Thus, the blocking of pathogenic epitopes using engineered Fabs appears to demonstrate efficacy and may lead to disease-specific treatments for antibody-mediated autoimmune diseases. *(Am J Pathol 2010, 176:914–925; DOI: 10.2353/ajpath.2010.090744)*

Autoimmune diseases are a major cause of morbidity and mortality in humans, affecting approximately 5% of the general population.[1] In recent years, significant advances have been made in our understanding of autoimmune disease pathomechanisms, especially the roles of autoantibodies, complement system, and autoresponsive T cells. For many autoimmune diseases such as systemic lupus erythematosus, rheumatoid arthritis, anti-phospholipid syndrome (APS), and bullous pemphigoid (BP), complement activation is increasingly recognized as critical to tissue injury.[2–6] Studies of APS and BP, for example, showed that the classical pathway of complement activation is required for the development of tissue injury, although alternative pathways may also be involved.[4,7–9]

BP is the most common autoimmune blistering skin disease. Autoantibodies against collagen XVII (COL17) bind to dermal–epidermal junction (DEJ) components and activate the complement system that mediates a series of inflammatory events including dermal mast cell degranulation and generation of eosinophil-rich infiltrates, resulting in skin blister formation.[10–12] APS is a condition characterized by recurrent miscarriage and thrombosis formation in the presence of anti-phospholipid autoantibodies, and a therapy has been proven effective to prevent the fetal loss by using heparin to inhibit anti-phospholipid antibody–induced complement activation.[7,13,14] In both BP and APS, $F(ab')_2$ fragments from the pathogenic autoantibodies, which lack the Fc portion necessary to activate the complement pathway, fail to initiate the disease.[4,7] This suggests that preventing complement activation by blocking the binding of autoantibodies to the corresponding antigens can be a viable novel therapeutic strategy for treating these diseases.

Supported by a grant-in-aid from the Program for Promotion of Fundamental Studies in Health Sciences of the National Institute of Biomedical Innovation (NIBIO; to H.S.).

G.W. and H.U. contributed equally to this work. A.S. and H.S. contributed equally to the direction of this study.

Accepted for publication October 7, 2009.

Supplemental material for this article can be found on *http://ajp.amjpathol.org*.

Address reprint requests to Dr. Akihiko Shibaki or Dr. Hiroshi Shimizu, Department of Dermatology, Hokkaido University Graduate School of Medicine, N15 W7, Sapporo, 060-8638 Japan. E-mail: ashibaki@med.hokudai.ac.jp or shimizu@med.hokudai.ac.jp.

Table 1. PCR Primers for the Amplification of Human Antibody Gene Repertoires

Primers for κ	
HK5	5′-GAMATYGAGCTCACSCAGTCTCCA-3′ (Sac I)
HK3	5′-GCGCCGTCTAGAACTAACACTCTCCCCTGTTGAAGCTCTTTGTGACGGGCAAG-3′ (Xba I)
Primers for λ	
HL5	5′-CASTYTGAGCTCACKCARCCGCCCTC-3′ (Sac I)
HL3	5′-GAGGGATCTAGAATTATGAACATTCTGTAGG-3′ (Xba I)
Primers for Fd	
H135	5′-CAGGTGCAGCTGGTGSAGTCTGG-3′
H2	5′-CAGGTCAACTTGAAGGAGTCTGG-3′
H4	5′-CAGGTGCAGCTGCAGGAGTCGGG-3′
VH5	5′-CAGGTGCAGCTCGAGSAGTCTGG-3′ (Xho I)
HG3	5′-GCATGTACTAGTTTTGTCACAAGA-3′ (Spe I)

To allow for sequence variability, representative choices of wobble nucleotides were included in the primers (M = A/C, K = G/T, R = A/G, S = C/G, Y = C/T). Fd fragments of human IgG were amplified in a two-step procedure. First, antisense primers H135, H2, and H4 were combined with HG3 for the amplification of heavy chain genes from human VH1–VH5 families and the *Spe* I site was introduced. In the second step, antisense primer VH5 was combined with HG3 to reamplify the heavy chain genes and introduce the *Xho* I site. Underlined sequences are restriction sites for the enzymes indicated in parenthesis.

The purpose of this study is to provide a proof of concept for this new strategy of treating antibody-mediated autoimmune disorders by using recombinant Fabs to block complement activation induced by pathogenic autoantibodies. Toward this end, we use BP as an example of a typical autoimmune disease. Our group has recently established a BP mouse model using a newly constructed COL17 humanized mouse.[3] Here we report our success in developing Fabs against the noncollagenous 16th-A domain (NC16A) of COL17, the main pathogenic epitope of BP autoantibodies,[15] for the blockade of autoantibody-initiated BP disease.

Materials and Methods

Construction of Phage Antibody Libraries

We constructed two individual Fab phage libraries from mononuclear cells isolated from two patients with active BP. The diagnosis of BP was made by the typical clinical and histological manifestations as well as by laboratory data including anti-COL17 ELISA and indirect immunofluorescence (IIF). Phagemid expression vector p3MH, a gift from Dr. Yan Wang (Central Lab of Navy General Hospital, Beijing, China), was derived from pCOMB3H (Scripps Research Institute, La Jolla, CA) by adding 9E10/c-*myc* epitope for detection and a hexahistidine tag for column purification at the 3′ end of Fd.[16] Using previously described methods and a set of PCR primers (Table 1),[17–19] antibody genes were amplified by RT-PCR from approximately 1×10^8 mononuclear cells isolated from 50 ml of peripheral blood from each patient. The phage antibody libraries were constructed by randomly combining the genes coding Fd fragments of IgG heavy chains with IgG light chain genes of either lambda or kappa DNA in equal amounts (see Supplemental Figure S1 at http://ajp.amjpathol.org.). The phagemid libraries were electroporated into *E. coli* XL1-Blue strain (Stratagene, La Jolla, CA), and the phage display of the libraries was performed as described elsewhere.[17,20] Before amplification, the resulting libraries were examined for the coexpression of heavy and light chains by enzyme digestion and for the diversity by fingerprinting of antibody genes (Fd and light chain) of 24 randomly selected single colonies.[20,21] The amplified recombinant phages were purified from culture supernatants by polyethylene glycol precipitation and resuspended in PBS, pH 7.4, containing 1% bovine serum albumin (BSA) and 10% glycerol.

Isolation of Phage Antibodies against NC16A Domain of Human COL17

Recombinant fusion peptide of the human COL17 NC16A domain (rhNC16A) with glutathione S-transferase (GST) was synthesized as reported previously.[3] Library panning was performed routinely.[20–22] Briefly, a freshly amplified phage library (approximately 1×10^{12} phages) was incubated for 2 hours at 37°C in immuno-tubes (Nunc, Roskilde, Denmark) coated with 50 μg/ml rhNC16A in 50 mmol/L $NaHCO_3$ pH 9.6. After washing of the tube with 0.05% (v/v) Tween-20 in PBS, adherent phages were eluted with 0.1 mol/L triethylamine (Sigma-Aldrich, Inc., St. Louis, MO). After neutralization with 1 mol/L Tris, pH 7.4, eluted phages were used to infect a fresh culture of XL1-Blue *E. coli*, which was amplified overnight as previously described.[20] Phages were harvested from culture supernatants and then repanned against rhNC16A for three subsequent rounds as described for the original library. Individual single ampicillin-resistant colonies resulting from infection of *E. coli* XL1-Blue with the eluted phage from the fourth panning round were isolated, and the binding to rhNC16A was confirmed by ELISA using HRP-conjugated anti-M13 mAb (Amersham Biosciences UK Ltd., Little Chalfont, Buckinghamshire, UK) as the developing reagent. The specific binders were screened by gene fingerprinting and sequencing to identify different clones. The variable region sequences of the separate selected clones were analyzed for homology to known human V, D, and J genes using the V BASE database (http://vbase.mrc-cpe.cam.ac.uk/).

Production, Purification, and Characterization of Soluble Fab

Fab Production and Purification

Plasmid DNA of the distinct selected clones was prepared, digested by *Nhe*I (New England BioLabs,

Ipswich, MA) to remove the gene III fragment, self ligated, and transformed into *E. coli* XL1-Blue. Clones were grown in LB containing 100 μg/ml ampicillin, and Fab expression was induced using 1 mmol/L isopropyl β-D-thiogalactopyranoside (IPTG, Sigma) in culture grown at 30°C overnight. Cells were pelleted by centrifugation, and the supernatant containing soluble Fab was taken for analysis.

Large-scale production of Fabs was achieved by growing Fab-express clones in *E. coli* XL1-Blue in 1 L of LB (plus 100 μg/ml ampicillin). Protein production was then induced with 1 mmol/L IPTG by culturing overnight at 30°C at 240 rpm. The culture supernatant was harvested by centrifugation. Fab purification was performed using HisTrap FF crude column (GE Healthcare Bio-Sciences AB, Uppsala, Sweden) according to the manufacturer's instructions. The purified Fabs were dialyzed against PBS and concentrated by Amicon ultrafiltration (Millipore, Lexington, MA) and were then characterized by SDS-PAGE and Western blotting. For animal experiments, the concentration of endotoxin in the purified Fabs was detected with the limulus amoebocyte lysate test using the QCL-1000 kit (Cambrex Bio Science Walkersville, Inc., Walkersville, MD), and endotoxin removal was performed by using Detoxi-Gel AffinityPak column (Pierce, Rockford, IL), where necessary.

ELISA

The binding activity and specificity of Fabs was confirmed by ELISA assay. ELISA plate wells were coated with 5 μg/ml rhNC16A in 50 mmol/L $NaHCO_3$ pH 9.6. Recombinant mouse NC16A (rmNC16A), GST, and BSA were used as negative control antigens at similar concentrations. Supernatant containing Fabs or appropriately diluted purified Fabs was incubated on ELISA plates. After washing, plates were developed with HRP-conjugated mAbs to human lambda light chain (Kirkegaard & Perry Laboratories, Gaithersburg, MD) or kappa light chain (Bethyl Laboratories, Inc., Montgomery, TX) and o-phenylenediamine substrate (Wako, Osaka, Japan). Absorbance was read at 492 nm.

Western Blotting

Western blotting was performed as previously described. Briefly, recombinant proteins were electrophoresed on SDS-PAGE and electrotransferred onto nitrocellulose membrane. The blots were blocked with 5% milk in TBS/T and incubated for 1 hour with the diluted Fabs at room temperature. After washing, the blots were incubated with HRP-conjugated mAbs to human lambda light chain or kappa light chain. The bound antibodies were detected by the Phototope Western Detection Systems (Cell Signaling Technology, Inc., Danvers, MA).

Epitope Mapping

Epitope mapping studies were performed using the standard Western blotting protocol described above. The NC16A domain of human COL17 was divided into subregions as described by Giudice et al.[15,23] The expression vectors NC16A1, NC16A2, NC16A2.5, and NC16A3, which respectively correspond to amino acid segments 490 to 506, 507 to 520, 514 to 532, and 521 to 534, were gifts from Dr. George J Giudice (Medical College of Wisconsin, Milwaukee). Affinity purified products of recombinant human NC16A and its subregions were electrophoresed and electrotransferred to nitrocellulose membrane. The membranes were then probed with Fabs and allowed to react with HRP-conjugated secondary mAbs to human lambda light chain or kappa light chain.

Immunogold Electron Microscopy

Normal human skin samples were processed for postembedding immunoelectron microscopy as previously described.[24,25] Briefly, cryofixed cryosubstituted samples were embedded in Lowicryl K11M resin and polymerized at −60°C under UV light. Selected blocks were used to produce ultrathin sections that were incubated with Fabs (80 μg/ml), diluted in PBS-based buffer, and washed four times (five minutes each). Further incubations were performed using rabbit anti-c-*myc* tag antibody (Santa Cruz Biotechnology, Santa Cruz, CA) followed by four washes and further incubation with 5-nm gold-conjugated antibody for immunogold labeling (Biocell, Cardiff, UK) diluted 1 in 200 in TBS buffer. Other primary anti-COL17 antibodies included for comparison were HD4 233, 1D1, and 1A8C, each of which recognizes different domains of human COL17 (extracellular domain close to the C-terminal, mid portion, and cytoplasmic domains, respectively).[26] Sections were viewed under a Hitachi H-7100 transmission electron microscope (Hitachi, Tokyo, Japan) at 80 KV.

Immunofluorescence

Five-μm cryosections of OCT-embedded skin were cut and placed onto microscope slides and subjected to IF studies. IIF using Fabs was performed on the skin samples from human or COL17 humanized mice using a standard protocol. FITC conjugated secondary antibodies against human lambda light chain (DakoCytomation, Glostrup, Denmark), kappa light chain (Invitrogen Corp., Carlsbad, CA), or c-*myc* tag (Santa Cruz Biotechnology) were used as detection reagents.

Surface Plasmon Resonance Analysis

Affinity of the generated Fabs was determined by BIAcore assay. The on and off rate constants (k_{on} and k_{off}) for binding of the Fabs to rhNC16A were determined by a BIAcore 2000 instrument (Biacore AB, Uppsala, Sweden). For analysis of the interaction kinetics, Fabs in various concentrations (100, 80, 60, 50, and 40 nmol/L) were injected over the immobilized antigen at a flow rate of 20 μl/min using HBS-EP buffer (Biacore AB). The association and dissociation phase data were fitted simultaneously to a 1:1 Langmuir global model by using the

BIAevaluation software. The affinities (dissociation constant, K_D) were calculated from the ratio of the rate constants of association and disassociation (k_{on}/k_{off}).

Functional Analysis of Fabs in Vitro

Preparation of BP Autoantibodies

BP autoantibodies were purified from either pooled sera from 20 patients or were included as separate serum samples from three patients with active BP. Briefly, the total IgG fraction from BP sera was prepared by affinity chromatography using HiTrap Protein G HP column (Amersham Biosciences UK Limited). Then, BP autantibodies against the COL17 NC16A peptide were affinity purified from the IgG fraction using HiTrap NHS-activated HP column (Amersham Biosciences UK Ltd.) precoated with rhNC16A according to the manufacturer's instructions.[3] The NC16A affinity purified BP autoantibodies were dialyzed against PBS and concentrated by Amicon ultrafiltration (Millipore). These NC16A affinity purified BP autoantibodies were designated as BP antibodies (BPAbs), and used for *in vitro* inhibition experiments.

For the *in vivo* experiments using whole BP-IgG fractions as the pathogenic autoantibodies, serum samples were collected from another 10 BP patients and total IgG fraction was prepared using HiTrap NHS-activated HP column. This was designated as BP-IgG. Binding activity with different autoantigens was tested by ELISA and Western blotting. The BP-IgG from all ten of the serum samples bound to human COL 17, and the BP-IgG from seven of the ten serum samples also reacted with BP230. The binding of the BP-IgG with the subdomains of NC16A (NC16A-1, -2, -2.5, -3, as described by Giudice et al[15]) was further studied. All ten of the serum samples bound to NC16A-2 and NC16A-2.5. In addition, two of the ten serum samples also bound to NC16A-1 or -3. When the pooled IgG from these ten patients was first incubated with the NC16A domain of COL17 overnight at 4°C, the reaction with the NC16A domain was markedly reduced, whereas binding to the full length COL17 was unchanged by Western blotting. This indicates that the BP-IgG recognize numerous epitopes on both COL17 and BP230 antigens, and that there exist autoantibodies recognizing different epitopes both within and outside of the COL17 NC16A domain.

Inhibition ELISA

To check the competition effect of Fabs on the binding of BPAbs to rhNC16A, an inhibition ELISA was performed by incubating purified BPAbs (8 μg/ml) with 0 to 32 μg/ml Fabs on rhNC16A ELISA plates. To detect the IgG autoantibodies, the plates were developed with HRP-conjugated polyclonal antibody to human IgG (DakoCytomation) and o-phenylenediamine substrate. Absorbance was read at 492 nm. The reduced reaction of BPAbs with rhNC16A was expressed as an inhibition rate, which was calculated according to the following formula: inhibition rate % = (A492*b* − A492*f*)/A492*b* × 100, where A492*b* is the reaction with BPAbs only and A492*f* is the reaction competed with Fab at a given concentration.

Inhibition ELISA between phage antibodies (Phabs) and Fabs from the isolated clones was performed to determine whether the Fabs against different epitopes mutually cross-inhibit binding by steric hindrance. Individual Phabs were incubated with rhNC16A on ELISA plates. The reaction was challenged with Fabs from different clones at various concentrations. After washing, the remaining binding of the Phabs to rhNC16A was developed with the HRP-conjugated anti-M13 antibody and o-phenylenediamine substrate.

Inhibition IF

Inhibition IF was assessed to check the competition of Fabs to the binding of BPAbs by incubating purified BPAbs (10 μg/ml) with 0 to 40 μg/ml Fabs on human skin sections. FITC-conjugated anti-human IgG (DakoCytomation) was the detection reagent. The inhibition IF was also performed by sequential incubation with BPAbs on human skin sections, which was followed by Fabs with a 30-minute interval. The effects of Fab inhibition on the binding of autoantibodies from patients with linear IgA bullous dermatosis and anti-p200 pemphigoid were also observed.

In Vitro *Inhibition of BPAb-Induced Complement Activation*

BPAb-induced complement activation in human skin samples and the inhibitory effects of anti-COL17 NC16A Fabs were observed by IF as described by Nelson et al with minor modifications.[9] Cryosections of normal human skin were incubated with BPAbs (10 μg/ml), anti-COL17 NC16A Fabs (10 to 40 μg/ml), or BPAbs plus anti-COL17 NC16A Fabs for one hour at 37°C. Freshly prepared normal human serum was then added as a complete complement source. One hour after incubation, *in situ* deposition of human C1q and C3 at the DEJ was detected with FITC-conjugated mAbs to human C1q and human C3 (DakoCytomation), respectively.

Effects of Fabs on BP Mouse Model in Vivo

All mouse procedures were approved by the Institutional Animal Care and Use Committee of Hokkaido University, and the experimental mice were housed in a specific pathogen-free animal facility. The BP model mice were produced by injecting BP autoantibodies, either NC16A affinity purified BPAbs (50 μg/g body weight) or whole BP-IgG (1 mg/g body weight) prepared from BP patients, into the COL17 humanized neonatal mice, as previously reported.[3] At 48 hours after the injection, the mice developed human BP-like clinical and histological characteristics with serum autoantibody titers ranging from 1:80 to 1:640 in IIF and a mean BP180 antibody index value of 55.7 ± 21.1 by ELISA measurement, which is similar to the autoantibody level usually found in the sera of active BP patients. To observe the effects of the generated

anti-COL17 NC16A Fabs on the COL17 humanized mice and on the BPAb-induced disease, we divided the neonatal mice into different groups. We first injected Fabs from the three individual clones to test whether the recombinant Fabs themselves are pathogenic in COL17 humanized mice. The Fab doses were 30 to 90 μg/g body weight (30 μg/g body weight is roughly an equimolar dose compared with 50 μg/g body weight of IgG-BPAbs). To sequentially monitor the serum Fab levels after injection, 60 μg/g body weight of Fab-B4 was injected into the neonatal mice and blood samples were collected by sacrificing mice at 6, 24, 48, and 72 hours. The Fab concentration was quantified using a sandwich ELISA technique with two mAbs. To capture Fabs in the samples, rabbit anti-c-*myc* mAb (Santa Cruz Biotechnology) was coated onto ELISA plates (20 μg/ml in PBS overnight at 4°C). After blocking with 3% BSA for one hour at 37°C, individual serum samples were diluted with 1% BSA in PBS buffer (1:10) and incubated for 1 hour at 37°C. Purified Fab was used as a standard at concentrations ranging between 0.1 μg/ml and 50 μg/ml. The plate was then incubated with HRP-conjugated mouse anti-human lambda light-chain mAb to detect the reaction. The concentrations of Fabs in the samples were calculated from the standard curve for each plate.

The effects of Fabs on the BP autoantibody-induced mouse model were observed by injecting Fabs either from individual clones or from various combinations of the clones. The injection of antibodies into mice was performed as described previously, with minor modifications.[3] Briefly, each mouse received a single intraperitoneal injection of different antibodies according to group. At 48 hours after injection, the extent of skin disease was judged, including distinct Nikolsky sign. The animals were then sacrificed, and skin samples were studied by light microscopy and direct immunofluorescence microscopy using FITC conjugated antibodies against human lambda light chain (DakoCytomation), c-*myc* tag (Santa Cruz Biotechnology), human IgG (Jackson, West Grove, PA), and mouse complement C3 (Cappel, ICN Pharmaceuticals, Inc., Aurora, OH). The quantification of mast cells (MCs) and MC degranulation was performed as described by Nelson et al, and the results were expressed as a percentage of degranulated MCs (number of degranulated MCs per total number of MCs in 5 random fields × 100%).[9]

Blood was collected, and the serum sample was prepared and used for ELISA to determine the titers of circulating BPAbs or Fabs. The level of BPAbs in the serum samples of experimental mice was tested using an anti-COL17 ELISA kit according to the manufacturer's instructions (MBL, Nagoya, Japan). Absorbance was read at 450 nm. The index value was defined by the following formula: index = (A450 of tested serum − A450 of negative control)/(A450 of positive control − A450 of negative control) × 100. The concentration of the recombinant Fabs in serum samples obtained from the experimental mice was quantified using the sandwich ELISA technique described above.

Statistical Analysis and Ethical Considerations

Differences in the ELISA inhibition results among various groups were examined for statistical significance using the analysis of variance with Fisher PLSD test. For the analysis of MC degranulation among various groups of Fab treatments, we determined statistical significance using multiple tests including the Student *t* test and one way analysis of variance. *P* values less than 0.05 were considered significant.

This study was approved by the Institutional Review Board of Hokkaido University, and fully informed consent from all patients was obtained for use of human material.

Results

Isolation of Anti-COL17 NC16A Antibodies from Phage Antibody Libraries

Two individual Fab phage libraries containing 8×10^7 clones and 4×10^7 clones, respectively, were successfully constructed by combining light chain genes and heavy chain genes amplified from antibody repertoires of two BP patients (library 1 from patient 1; library 2 from

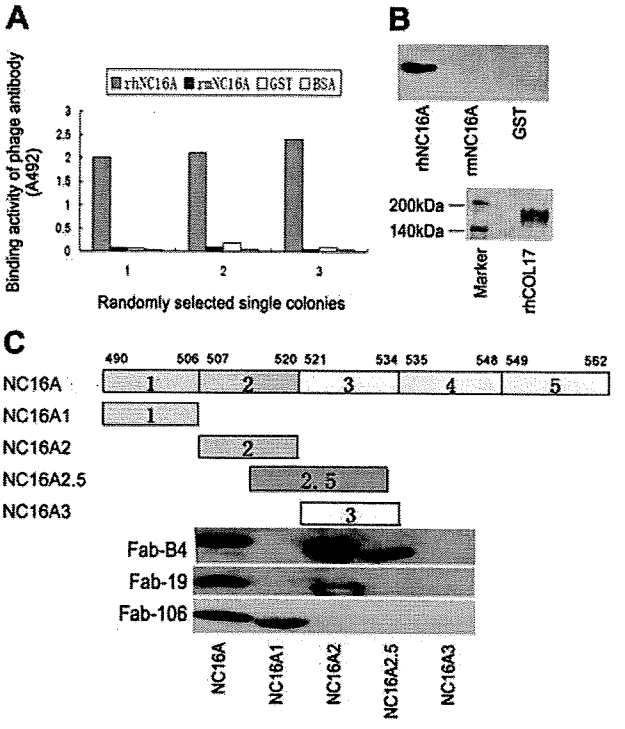

Figure 1. Isolation of specific binders against the NC16A domain of human type XVII collagen from phage antibody library. **A:** Randomly selected single colonies from the fourth panning round of the libraries show positive reaction with recombinant human NC16A (rhNC16A) but no reaction with recombinant mouse NC16A (rmNC16A), GST, or BSA in ELISA. **B:** Western blotting of soluble Fabs shows staining of only the rhNC16A domain and full-length human COL17, whereas rmNC16A and GST are negative. The representative results using Fab-B4 are shown. **C:** Epitope mapping of the generated Fabs with rhNC16A and its subdomains are shown. Fab-B4 binds to rhNC16A, NC16A2, and NC16A2.5 but does not react with NC16A1 and NC16A3, indicating that the binding epitope is located within an overlapping region within subdomain 2 and 2.5 (amino acids 514 to 520). The Fab-106 and Fab-19 epitopes are located in subdomain 1 (NC16A1, amino acids 490 to 506) and subdomain 2 (NC16A2, amino acids 507 to 520), respectively.

Table 2. Heavy and Light Chain Genes of Isolated Fabs

Fab clone	VH family	Amino acid sequences of VH			VL family	Amino acid sequences of VL		
		CDR1	CDR2	CDR3		CDR1	CDR2	CDR3
B4	VH1	NYAFSW	GIIPMSGEGHKAQKFQG	PSRSNYAGGMDV	Vλ1	SGSSSNIGRHYVY	TNYRRPS	ASWDDSL
B12	VH3	SYSMN	SISSSSSYIYYADSVKG	IDSSSWYEGWFDP	Vλ1	SGSTSNIGSNTVN	SNNQRLS	GTWDDSLN
B21	VH3	SYVLS	LLVVMLEADTTQTPEG	GNNWYGQTFDF	Vλ1	GAAPTSGQVMMYTW	GNSNRPS	QSYDSSLS
F32	VH3	SYAMH	VISYDGSNKYYADSVKG	ALRGYSYGT	Vκ1	RASQSISSYLN	AASSLQS	QQSYSLF
19	VH3	NYGMH	VISYDGSKKYYADSVKG	GFYYDWGTYYDY	Vλ1	TGSSSNIGAGYDVH	ANSNRPS	QSYDSSLT
106	VH3	DSAIH	RVRSKTNNYATDYAVSVKGR	HGESRSWYVGSGYWFDP	Vλ1	SGSSSNIGNNYVS	DNNKRPS	GTWDSSLS

Six unique antibody clones against the NC16A domain of human COL17 were identified by sequencing the heavy and light chain variable regions. Of these, clones B4, B12, B21, and F32 were isolated from library 1, whereas clones 19 and 106 were isolated from library 2. The deduced amino acids sequences of the complementary determining regions (CDRs) are shown.

patient 2). Phabs were selected by panning against rhNC16A immobilized on immune tubes. ELISA of the Phabs revealed specific positive reactions with rhNC16A in 40 of 96 and 32 of 80 colonies isolated from the two libraries, respectively (Figure 1A). By BstN I fingerprinting and sequencing of variable regions of heavy chain (VH) and light chain (VL) genes, nine unique antibody clones against rhNC16A were identified and were allowed to express the soluble Fab fragments.

Expression and Characterization of Fabs

Soluble Fab fragments of the nine antibody clones were successfully expressed by removing the gene III fragment of the phagemid vector. Four of the soluble Fabs from library 1 (Fab-B4, Fab-B12, Fab-B21, Fab-F32) and two from library 2 (Fab-19, Fab-106) were highly specific to rhNC16A in ELISA (data not shown) and Western blot analysis (Figure 1B, representative Western blot result). The other three clones, however, could not be detected as soluble fragments, probably because of their low affinity. The VH and VL genes of the six positive Fab clones are summarized in Table 2.

By epitope mapping, the binding site of the Fabs with rhNC16A and its subdomains was obtained. All four of the Fabs from library 1 showed the same reactive pattern. They bound to rhNC16A and subdomains 2 and 2.5 but failed to react with subdomains 1 and 3, indicating that their binding epitope was within the overlapping region (amino acids 514 to 520) of subdomains 2 and 2.5. The two Fabs from library 2 bound to different subdomains: Fab-106 reacted only with subdomain 1 (amino acids 490 to 506) and Fab-19 reacted only with subdomain 2 (amino acids 507 to 520). This indicates that they bound to different epitopes on COL17 NC16A. The representative blot results are shown in Figure 1C. These data demonstrate the successful isolation of anti-COL17 NC16A Fabs from patients with BP.

We chose Fabs (Fab-B4, Fab-19, and Fab-106) that had been raised against different epitopes of COL17 NC16A for further experiments. All of the light chains of these three clones are from human lambda light chain family. Large-scale production was performed, and a yield of approximately 1 to 3 mg of Fab product was obtained from each 1 L culture after column purification. Figure 2A shows the SDS-PAGE identification of the purified Fab in reduced and nonreduced form.

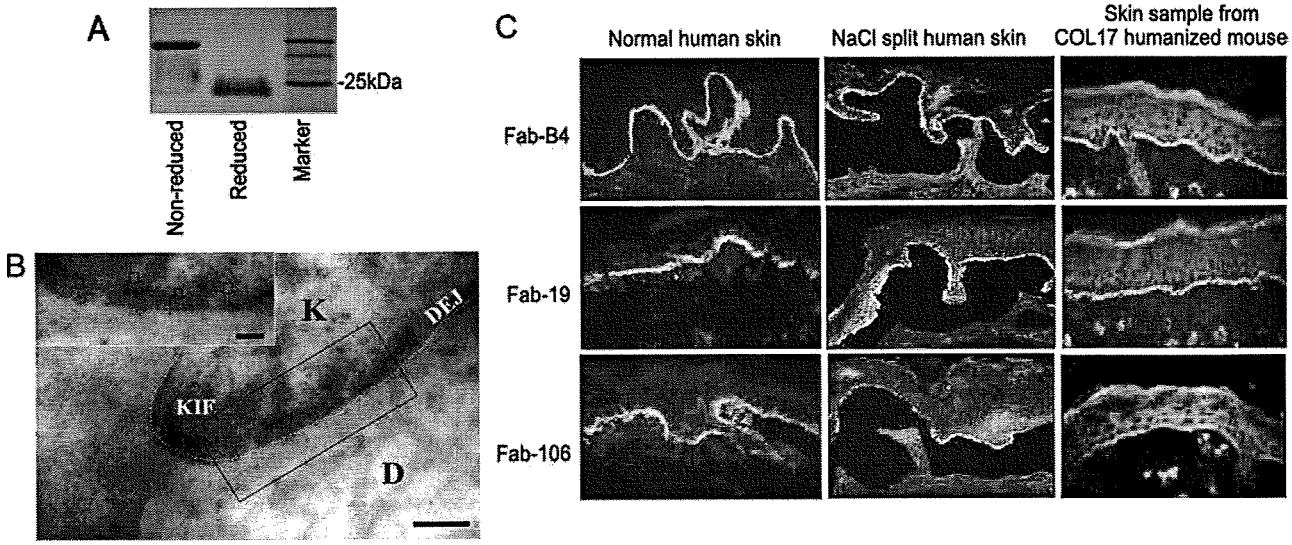

Figure 2. Production and characterization of Fabs. **A:** A purified soluble Fab in both reduced and nonreduced states is shown by Coomassie blue staining after SDS-PAGE. **B:** Immunogold labeling of normal human skin by Fabs shows 5-nm immunogold deposits restricted to immediately beneath hemidesmosomes, close to the keratinocyte plasma membrane (**arrows**, bar = 100 nm). The representative results using Fab-B4 are shown. (**K:** keratinocyte; **D:** dermis; KIF: keratin intermediate filaments; DEJ: dermal-epidermal junction). **C:** Immunofluorescence studies on normal human skin and skin sections from COL17 humanized mice show positive staining of the selected Fabs at the DEJ, and positive staining is also noted on the roof of NaCl split skin samples.

Table 3. Affinity of Anti-COL17 NC16A Fabs Measured by BIAcore System

Fab	k_{on} (1/Ms)	k_{off} (1/s)	K_D (M)
Fab-B4	2.83×10^5	1.10×10^{-3}	3.89×10^{-9}
Fab-19	1.14×10^5	6.26×10^{-3}	5.48×10^{-8}
Fab-106	5.52×10^5	8.08×10^{-2}	1.46×10^{-7}

Kinetic parameters k_{on} and k_{off} were measured by BIAcore system, and K_D was calculated as k_{on}/k_{off}. From the three Fabs, Fab-B4 has the highest affinity.

Immunogold electron microscopy showed that 5-nm immunogold particles were restricted to immediately beneath hemidesmosomes, below the keratinocyte plasma membrane (Figure 2B). Mean measurements of immunogold deposits demonstrated that their epitopes were about 1 to 2 nm (mean 1.77 nm ± SD, $n > 200$) beneath the plasma membrane and located between the epitopes of 1A8C, a cytoplasmic plaque associated COL17 antibody) and 233 (an extracellular COL17 antibody), as described by Nonaka et al.[26] No difference in distribution of the immunogold deposits was found between the three Fabs.

In the IIF experiments, as we expected, all three Fabs showed linear deposition at the DEJ and positive staining was noted along the roof of the NaCl split skin samples, consistent with COL17 staining (Figure 2C).

Kinetic analysis using the BIAcore system demonstrated affinity levels of Fab-B4, Fab-19, and Fab-106, as summarized in Table 3. Among these Fabs, Fab-B4 showed the highest affinity value and Fab-106 showed the lowest.

Functional Analysis of Fabs in Vitro

To determine whether the Fabs generated against COL17 NC16A were able to function in competitive binding to inhibit the emergence of an autoantibody-mediated BP phenotype, we initially performed a series of *in vitro* experiments to evaluate their ability to block BP autoantibody binding to COL17. Figure 3A shows that the rhNC16A binding activities of BPAbs, which were affinity purified using recombinant COL17 NC16A peptide from the pooled sera from 20 BP patients, were reduced markedly and significantly by Fab-B4 and Fab-19, but only marginally by Fab-106, in a dose-dependent manner (0 to 32 μg/ml). Fab-B4 and 19 suppressed the binding of BPAbs most efficiently at a concentration of 32 μg/ml, with the highest inhibition rates of 52.4% and 50.8%, respectively. Combinations of two or three Fabs failed to increase this inhibition efficacy. When tested with BPAbs isolated from individual BP patients, Fabs showed similar competitive effects (Figure 3B).

IIF studies show competitive blocking of Fabs with BPAbs on skin sections. Figure 4 shows positive IgG

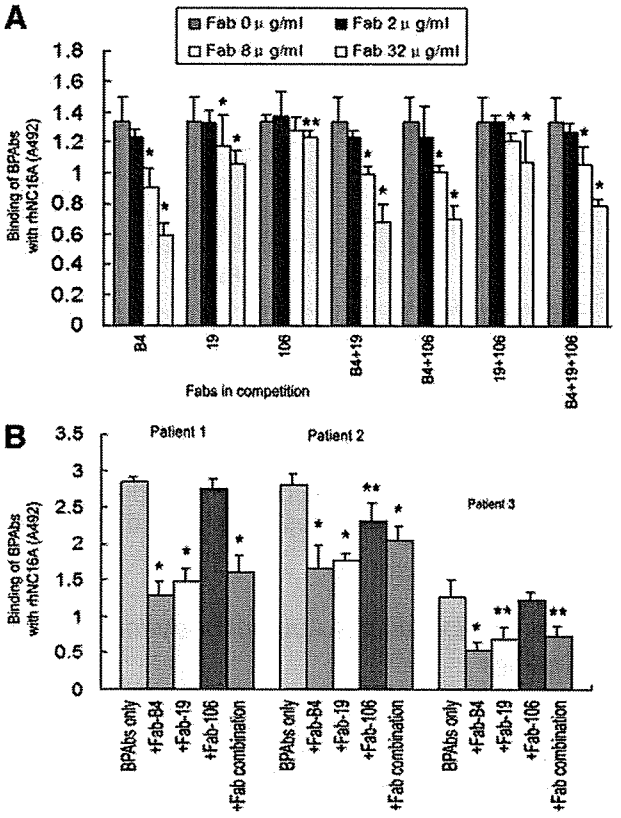

Figure 3. Inhibition ELISA assay. **A:** The effects of competition with Fab-B4, Fab-19, and various combinations inhibit the binding of autoantibodies (BPAbs, 8 μg/ml) from pooled sera of patients with bullous pemphigoid (BP) to rhNC16A in a dose-dependent manner (0 to 32 μg/ml), whereas Fab-106 inhibits BPAb binding only moderately. $^*P < 0.01$, $^{**}P < 0.05$, versus the original binding of BPAbs. **B:** Fabs (32 μg/ml) inhibit the binding of BPAbs from three BP patients. $^*P < 0.01$, $^{**}P < 0.05$, versus the original binding of BPAbs.

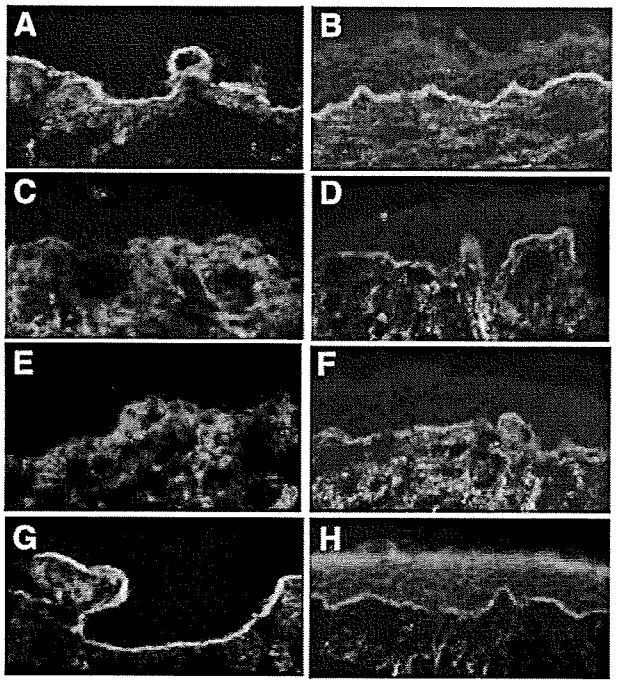

Figure 4. Inhibition immunofluorescence. **A** and **B:** Positive IgG staining of the NC16A affinity purified BPAbs (10 μg/ml) at the DEJ in human skin. **C** and **E:** IgG BPAbs staining is blocked by coincubation with either Fab-B4 or Fab-19 at a concentration of 20 μg/ml. **G:** Fab-106 (20 μg/ml) fails to significantly inhibit the binding of BPAbs. When BPAbs are allowed to bind to skin sections first and Fabs are added 30 minutes later, the IF staining of BPAb binding is also markedly reduced by Fab-B4 (**D**) or Fab-19 (**F**) but not by Fab-106 (**H**).

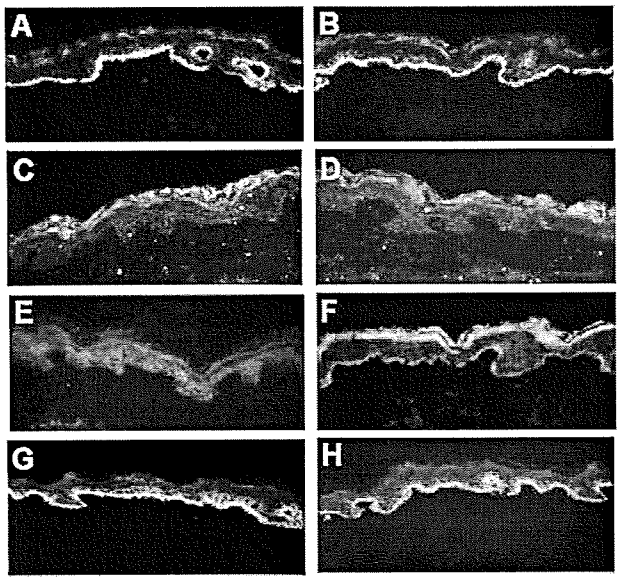

Figure 5. BPAb-induced complement activation and the inhibitory effects of Fabs. NC16A affinity purified BPAbs (10 μg/ml) induced activation of human C1q and C3 is shown at the DEJ in cryosections of human skin (**A** and **B**). When Fabs are coadministered with BPAbs at the same concentration, Fab-B4 completely blocks C1q and C3 activation (**C** and **D**), whereas Fab-19 effectively blocks the activation of C1q (**E**) and markedly reduces the activation of C3 (**F**). Fab-106 shows no inhibition of either C1q or C3 activation (**G** and **H**).

BPAbs staining (10 μg/ml) at the DEJ in human skin (Figure 4A), which was blocked by coincubation with either Fab-B4 or Fab-19 at a concentration of 20 μg/ml (Figure 4, C and E). Fab-106 failed to significantly inhibit the binding of BPAbs (Figure 4G). When BPAbs were allowed to bind to skin sections first and Fabs were added 30 minutes later, the IF staining of BPAb binding was also markedly reduced although not completely inhibited (Figure 4, B, D, F, and H). Competitive IF using Fabs and individual patient BPAbs showed that Fab-B4 and Fab-19 were able to block the binding of autoantibodies from three individual BP patients, whereas none of the Fabs inhibited the binding of IgA autoantibodies from patients with linear IgA bullous dermatosis or IgG autoantibodies from patients with anti-p200 pemphigoid (data not shown).

In vitro inhibition of complement activation by recombinant Fabs was studied by immunofluorescence. *In situ* deposition of BPAb-activated C1q (Figure 5A) and C3 (Figure 5B) was found at the DEJ in human skin. Complement deposition was reduced or completely blocked by Fab-B4 (Figure 5, C and D) or Fab-19 (Figure 5, E and F), whereas it was unchanged by Fab-106 treatment (Figure 5, G and H). Fabs against COL17 NC16A did not activate complement at concentrations up to 100 μg/ml.

We also tested the effect of competition between recombinant anti-COL17 NC16A Fabs. Using an inhibition ELISA, Fabs from the three clones inhibited the binding of Phabs from their own clone as we might have expected. Interestingly, Fab-B4 and Fab-19 cross-inhibited each other while Fab-106 failed to inhibit the other two (Figure 6, A–C). These data indicate that Fab-B4 and Fab-19 specifically recognize distinct but close or overlapping

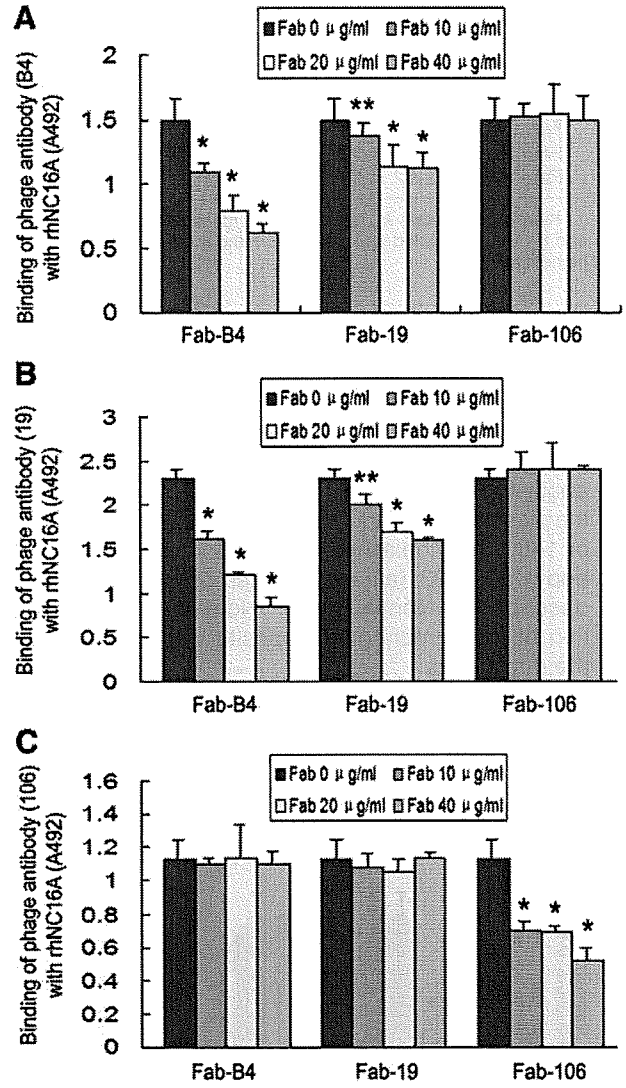

Figure 6. Inhibition ELISA for the three recombinant antibody clones using Fabs and phage antibodies (Phabs). Fab-B4 and Fab-19 inhibited the binding of both Phab-B4 and Phab-19 (**A** and **B**), whereas Fab-106 inhibited Phab-106 only (**C**). This indicates that the antibody clones B4 and 19 are mutually cross-inhibiting. $^{*}P < 0.01$, $^{**}P < 0.05$, versus the original binding of respective Phabs.

epitopes and are able to block the binding of BP antibodies in nearby epitopes, most likely by direct steric hindrance.

In Vivo *Blockade of Autoantibody-Induced BP Disease*

We first proved that recombinant Fabs were not pathogenic to COL17 humanized mice after injection with 30 to 90 μg/g body weight of Fab-B4, -19, or -106 into neonatal mice. Neither clinical signs, including erythema and Nikolsky sign, nor any histopathological manifestations of BP were found in the treated mice. Direct immunofluorescence studies demonstrated clear deposition of the recombinant Fab fragments at the DEJ. Subsequent deposition of mouse C3 was not detected (Figure 7A).